



Predicted wind and solar energy expansion has minimal overlap with multiple conservation priorities across global regions

Sebastian Dunnett^{a,b,1} , Robert A. Holland^{a,b} , Gail Taylor^{b,c} , and Felix Eigenbrod^a 

^aGeography and Environmental Science, Faculty of Environmental and Life Sciences, University of Southampton, Southampton SO17 1BJ, United Kingdom; ^bBiological Sciences, Faculty of Environmental and Life Sciences, University of Southampton, Southampton SO17 1BJ, United Kingdom; and ^cPlant Sciences, University of California, Davis, CA 95616

Edited by Monica Turner, Department of Integrative Biology, University of Wisconsin, Madison, WI; received March 11, 2021; accepted November 29, 2021

Protected areas and renewable energy generation are critical tools to combat biodiversity loss and climate change, respectively. Over the coming decades, expansion of the protected area network to meet conservation objectives will be occurring alongside rapid deployment of renewable energy infrastructure to meet climate targets, driving potential conflict for a finite land resource. Renewable energy infrastructure can have negative effects on wildlife, and co-occurrence may mean emissions targets are met at the expense of conservation objectives. Here, we assess current and projected overlaps of wind and solar photovoltaic installations and important conservation areas across nine global regions using spatially explicit wind and solar data and methods for predicting future renewable expansion. We show similar levels of co-occurrence as previous studies but demonstrate that once area is accounted for, previous concerns about overlaps in the Northern Hemisphere may be largely unfounded, although they are high in some biodiverse countries (e.g., Brazil). Future projections of overlap between the two land uses presented here are generally dependent on priority threshold and region and suggest the risk of future conflict can be low. We use the best available data on protected area degradation to corroborate this level of risk. Together, our findings indicate that while conflicts between renewables and protected areas inevitably do occur, renewables represent an important option for decarbonization of the energy sector that would not significantly affect area-based conservation targets if deployed with appropriate policy and regulatory controls.

renewable | energy | biodiversity | conservation

Given its contribution to greenhouse gas emissions, the global energy sector will be required to undergo a substantial transformation over the coming decades to combat climate change and meet ambitions laid out in the Paris Agreement (1). There is evidence that such a change is already occurring with global renewable energy generation capacity reaching $\sim 2,537$ GW in 2019, an increase of 7.4% on 2018. This trend will likely continue, with the International Energy Agency forecasting that renewable energy capacity may increase by over 50% by 2024 (2). Much of this growth is expected to occur in the wind and solar sectors (3).

Renewable energy technologies possess energy densities that are orders of magnitude below conventional fossil fuels (4–9). While coal and gas can reach power densities as high as 2000 Wm^{-2} , the most power-dense renewable technology (concentrating solar power [CSP]) peaks at just 10 Wm^{-2} (10). For this reason, there is increasing concern about the implications of the expansion of renewable energy for the global land system (11). While there has been a substantial focus on the land use implications of bioenergy expansion (12), with one forecast that an area the size of India will be required for energy crop production (13, 14), less attention has been given to other forms of renewable energy. This is an important omission; onshore wind energy could disrupt

up to $83,226 \text{ km}^2$ of land by 2050 (15), while solar photovoltaic (PV) and CSP have been shown to drive conversion of natural land cover in the United States (16).

The expansion of renewable energy and the associated increase in requirements for land may lead to conflict with other pressures on finite land resources, most notably with food production and biodiversity conservation. Based on a projection of future demand associated with factors such as changing diets and demographics, food production may need to increase by 100% of 2005 levels by 2050 (17). Although some of this increase can be achieved through improved agronomic practices and genetics, some expansion of agricultural land will undoubtedly be required, particularly as agricultural efficiency gains have stagnated (18, 19). Simultaneously, efforts to halt the loss of global biodiversity have led to calls for the existing Aichi Biodiversity Target 11, to protect at least 17% of global land area, to be expanded to a target of 30%, with some advocates suggesting that half of Earth's area should be protected in some way or other (20). Together, these issues represent a confluence of challenges for global sustainability: how to balance demands for energy, food production, and biodiversity within a finite land area.

This study examines the interactions between two of these sustainability challenges by considering whether renewable energy technologies, in the form of onshore wind and solar PV, represent an important stressor that will impact our ability to achieve area-based conservation targets to address biodiversity loss. Our analysis enables identification of areas where conflict currently exists and, more critically, where tradeoffs might occur in the future (21–25). This allows the direct local impacts of renewable energy, which are relatively well known (4, 9), to

Significance

Conservation scientists warn of the threat to area-based conservation posed by renewable energy infrastructure. Here, we show that the current and near-term overlap of the two land uses need not be as severe as previously suggested. This is important, as global efforts to decarbonize energy systems are central to mitigating against climate change and the strong negative impacts of projected climate change on biodiversity.

Author contributions: S.D. and F.E. designed research; S.D. performed research; R.A.H. and F.E. contributed new reagents/analytic tools; S.D. analyzed data; S.D. wrote the paper; R.A.H., G.T., and F.E. contributed revisions to the manuscript; and R.A.H., G.T., and F.E. wrote the grant application that funded the work.

The authors declare no competing interest.

This article is a PNAS Direct Submission.

This open access article is distributed under [Creative Commons Attribution-NonCommercial-NoDerivatives License 4.0 \(CC BY-NC-ND\)](https://creativecommons.org/licenses/by-nc-nd/4.0/).

¹To whom correspondence may be addressed. Email: sebdunnett@gmail.com.

This article contains supporting information online at <http://www.pnas.org/lookup/suppl/doi:10.1073/pnas.2104764119/-DCSupplemental>.

Published January 31, 2022.

be interrogated and potentially mitigated. Local impacts of renewables on biodiversity can be considerable; wind turbines have significant effects on volant species (26–29), while solar PV can also have significant local effects including vegetation removal and soil degradation (30–32).

Recent work (33) has demonstrated considerable overlap globally of renewable energy facilities and important conservation areas (defined as the combination of protected areas, Key Biodiversity Areas [KBAs], and wilderness areas), mainly in regions with high prevalence of both land uses (e.g., Western Europe). Wind power was found to overlap with the largest number of conservation areas. However, this study did not weight overlaps by areas—countries with large areas of both protected areas and renewables are likely to have higher absolute overlaps than countries with smaller areas of both land uses. More critically, major gaps remain in our ability to predict future conflict between wind and solar and protected areas (PAs) globally because of data limitations. Previous studies have examined potential future conflict using a variety of techniques including data on facilities under development as a proxy for future threat, using suitability layers based solely on resource availability, and multicriteria approaches combining resource availability with development feasibility (33–35). However, a lack of global harmonized data on wind and solar installations means that the assumption that renewable energy infrastructure can be predicted in these ways has not been systematically tested.

Here, we address current methodological shortcomings using an available dataset (36) that allows us to systematically examine whether renewable energy infrastructure represents a salient threat to area-based conservation. To answer this question, we investigate the spatial overlap of onshore wind and solar PV and important conservation areas, both following existing methods and after controlling for area. Secondly, we address shortfalls in previously used suitability-based approaches for predicting renewable energy expansion by using wind and solar data (36) to generate future development likelihood layers with random forest (RF) modeling. Finally, we combine our renewables likelihood surfaces with existing projections of future PAs (37) to assess the threat of future co-occurrence for renewables and PAs.

Results

Owing to data limitations, the results presented here do not provide a global picture; they instead aggregate results for nine regions of the world with sufficient renewable energy observations (*Materials and Methods*). In the first stage of our analysis, we investigate the spatial overlap of onshore wind and solar PV with important conservation areas, both following existing methods and after controlling for area. Standard spatial overlaps of renewable energy and important conservation areas using our harmonized data (*Materials and Methods*) (36) largely corroborate recent work (33): We find that 3,666 wind and solar PV installations out of a total of 24,624 (14.89%) occur within important conservation areas (*SI Appendix, Table S1*). We define important conservation areas following Rehbein et al. (33): PAs; KBAs, as defined by the Key Biodiversity Area Partnership; and wilderness areas, “areas free of industrial scale activities and other human pressures which result in significant biophysical disturbance,” as defined by Allan et al. (38). PAs and KBAs contain many of the overlapping installations (1,354 and 2,266), with wilderness areas containing 46 installations. Most overlaps occur in PAs with no official International Union for Conservation of Nature (IUCN) designation ($n = 367$). Although the next highest number of PAs containing installations are management categories V and VI, where limited development is allowed ($n = 169$), there are still overlaps in areas designated management category I to IV ($n = 52$), where no development

activity should occur (although the installations tend to be <100 megawatts; *SI Appendix, Fig. S1*). We also find that most conservation areas containing renewable energy installations (820, or 76.78%) occur in Europe (Northern, Central, and Southern) (*SI Appendix, Table S2*). Three of the seven wilderness areas containing renewable energy installations occur in North America (also the region with the largest area of wilderness globally, 8.513 million km²).

Since renewable energy infrastructure and PAs are not currently mutually exclusive, it is possible that absolute overlaps of renewable energy installations are likely to be higher as the area of installations (and conservation areas) increases. Indeed, historical overlaps suggest that this is the case, as the proportion of overlaps remain constant as both areas increase (*SI Appendix, Fig. S2*); looking at overlaps relative to area is therefore important, as there is a strong correlation between renewable energy overlap area and the amount of protected area per country (*SI Appendix, Table S3*; R^2_{adj} values of 0.3763 for PAs and 0.2904 for KBAs). We constructed simple linear regressions to assess the degree to which countries had more (or less) area of overlap (hereafter “relative overlap”) given the area of land, renewable energy, and conservation areas (*Materials and Methods*; *SI Appendix, Tables S6 and S7*). This shows that despite the large absolute number of overlaps in Europe, it is only Spain, Portugal, and France that show more overlap than expected relative to their respective areas. Outside of Europe, Brazil, Uzbekistan, and the United States all exhibit unusually high relative overlaps.

In documented instances in which overlaps do occur, we find little evidence that renewable energy infrastructure has led to instances of PAs being downgraded, downsized, or degazetted (so-called “PADDD events”). Downsizing describes the reduction in area of a protected site, downgrading the weakening of legal protection, and degazettement the complete loss of legal protection. There were only eight overlapping records of such events and renewable energy locations globally: six from validated PADDD polygons (all from the United States) and two from buffered point data (one from Canada and one from China). Although all instances were attributed the cause “Infrastructure,” none of the records appeared to be directly linked to renewable energy infrastructure development. The six records of overlap in the United States were all examples of PADDD associated with Bill H.R. 399 allowing the construction of infrastructure (roads, etc.) for border security. The Canadian PADDD event allows various forms of research to be conducted by industry (and others) for infrastructure development, while the Chinese record does not have associated metadata elaborating the cause of the area downsizing.

In the second analysis, we address shortfalls in previously used suitability-based approaches for predicting renewable energy expansion by using wind and solar data to generate future development likelihood layers. Our results demonstrate that existing state-of-the-art methods for predicting future wind and solar based on resource potential with development feasibility (development potential indices [DPIs]) (34) do not adequately capture the solar PV and wind estate in our study regions. DPIs for actual wind and solar installations did not differ substantially from an equal number of randomly located background points within our global dataset (36), signaling the DPIs are poor predictors of installation locations (*SI Appendix, Fig. S3*). We therefore used RFs to build probability of occurrence layers (RF potential [RFP] models) for wind and solar PV in select regions using a suite of global variables and our global dataset (*Materials and Methods*). These RFP models performed well, exhibiting a mean accuracy of 0.87 and mean κ of 0.731 for solar PV and 0.901 and 0.802, respectively, for wind. Importantly, RFP models in all regions also outperformed the DPIs when tested with an independent dataset of wind and solar infrastructure locations

(receiver operator characteristic curves in *SI Appendix, Fig. S4* and area under the curve values in *SI Appendix, Table S4*).

For solar PV, accessibility ranks highest for variable importance (*Materials and Methods*) for most RFP model regions (*SI Appendix, Fig. S5*); horizontal solar irradiance is largely unimportant for all regions except Central and Southern Europe and South Asia. Road density also appears to be an important predictor across most model regions. For wind, wind speed appears to be the most important predictor in all but Russia and the Balkans. Accessibility is not as universally important as with solar PV but still appears somewhat influential for all regions along with livestock density and wind speed.

Finally, we combine our renewables likelihood surfaces with existing projections of future PAs (37) to assess the threat of future co-occurrence for renewables and PAs. Bivariate plots of renewable likelihoods versus PA priority expansion rankings are presented in Fig. 1. From these, we isolate the top 30% of cells for expansion of each renewable technology and the top 30% of PA expansion rankings in Fig. 2. *Insets* for Figs. 1 and 2 show details for the US wind corridor, which already houses numerous wind installations; Germany, Europe's renewables powerhouse; urban China; and the high-biodiversity Atlantic forests of Brazil. High correlation between both wind and solar PV with PA priority expansion rankings can be seen in Fig. 1 in Germany and the Atlantic forests of Brazil. Different spatial distributions of wind and solar PV likelihood in the United States and China drive differences in priority overlaps between the two renewable technologies in these regions (Fig. 2).

Overlaps between RFP models of renewables and existing PA expansion rankings (37)—shown to be a good predictor of designations (*SI Appendix, Figs. S6 and S7*)—vary by region, priority threshold, and renewable technology (Fig. 3). Overlap ratios provide a summary of the spatial co-occurrence of two binary responses, accounting for differences in the areas of the responses; values >1 indicate over-representation given the areas, while values <1 indicate under-representation. Ratios here are calculated by dividing the percentage of PA priority cells that overlap priority renewable energy areas by the percentage of total land covered by priority renewable energy areas. These ratios are bound between 0 for complete spatial disaggregation (no overlap) and $1/x$ for perfectly overlapping priorities, where x is the percentage priority renewable energy area in a given region (e.g., 30% land devoted to renewables would provide an upper bound of 3.33, regardless of the area of PA priorities). A value of 1 would indicate no spatial relationship between PA priority expansion areas and priority renewable areas (*Materials and Methods* and graphical representation in *SI Appendix, Fig. S12*). For solar PV in Central Europe, when the PA priority expansion area is $>1\%$ (Fig. 3, *Top row excluding Leftmost plot*), PA priority expansion areas are already over-represented (i.e., overlap ratio >1) for even small areas of renewable priority. As renewable priority areas increase in coverage to 20%, the overlap ratio becomes even greater, suggesting that PAs and renewable priority areas spatially correlate in this range. Overall, however, overlaps between renewable energy priority areas and PA priority expansion areas tend to be either under-represented or representative of the wider landscape except for Central Europe and the Middle East for solar PV and the Middle East and Northern Europe for wind.

Discussion

Studies tend to suggest that the expansion of renewable energy is a de facto threat to biodiversity (24, 35); one warns that the number of active renewable energy facilities in important conservation areas could increase by 42% by 2028 (33). The results here suggest that existing studies may be overly pessimistic for our study regions. The reality is more nuanced: Future

expansion of renewables and PAs are both possible with relatively little overlap in these regions. Some measure of overlap should be seen as inevitable as available land diminishes for varying sustainability goals (39), and especially as a number of IUCN PA categories explicitly allow infrastructure development (40). Thoughtful planning of renewable energy installations may also alleviate some of the pressure on lands important for biodiversity (21, 22, 34, 41). However, our findings suggest that even in rapidly developing regions such as East and South Asia, PA priority expansion areas occur no more frequently in priority renewable energy areas than they do in the wider landscape (Fig. 3). Even in regions where the overlap ratio is significantly higher than one, indicating over-representation of overlapping areas (e.g., Europe and the Middle East), there still exists ample land within which to site renewable energy and PAs separately if appropriate policy and regulatory controls are employed. It is also important to note that the likely counterfactual to rapid deployment of renewable energy is not no additional energy infrastructure, but rather myriad energy scenarios, many including fossil fuels. Although fossil fuels are more energy dense in terms of their spatial footprint, they have been shown to impact priority conservation areas both directly through conversion, degradation, pollution, or disturbance of habitats and indirectly by increasing access for loggers, farmers, hunters, and settlements (42, 43). Furthermore, a continuation of reliance on fossil fuel energy has an extremely high likelihood of causing dangerous climate change (44, 45), which itself threatens the effectiveness of global PAs (46).

Our RFP models outperformed the previous DPIs at predicting wind and solar installations when applied to a different dataset than used to build the RFP models (*Materials and Methods; SI Appendix, Fig. S4 and Table S4*). This suggests the data used to build the RFP models adequately capture the biophysical and socioeconomic parameter space of predictors of these technologies and that our data-led approach, which includes a broader set of independent variables than previous approaches as well as their interactions, can help improve the identification of likely expansion areas. Furthermore, removing unnecessary land constraints—also seen in Santangeli et al. (35)—likely contributes to the improved performance of the RFP relative to the DPIs. Slope and elevation, for example, were relatively unimportant for RFP predictions despite their use as constraints for generating the DPIs. The difference between the approaches was notably more pronounced for solar than for wind. Onshore wind energy planning outcomes are strongly associated with the size of turbines and visual impact (47, 48), suggesting larger, remote wind projects are more likely to be developed. Larger projects may require maximization of resource efficiency to recoup significant capital costs, which may explain the disparity and why wind speed appears more important in the wind RFP model than irradiance in the solar model (*SI Appendix, Fig. S5*). Solar PV has, on average, a much smaller spatial footprint than wind ($0.07593 < 6.728 \text{ km}^2$; ref. 36) and is more likely to be accepted on poor quality agricultural land (47). This allows solar PV to be sited closer to existing electricity transmission networks, which may drive costs down so that they need not be recouped so aggressively by resource efficiency. Consequently, this makes solar PV less amenable to prediction by existing, resource availability-focused approaches.

The RFP layers depend heavily on the assumption that historic drivers of renewable energy predict its expansion. In rapidly changing socioecological conditions, past predictors of land use change are unlikely to remain relevant for long (49, 50). However, there are two reasons why we believe the predictors used in this study will remain stable in the near term (we define near term as the next several years to two decades). First, the renewable energy estate is still arguably in its infancy, and it is unlikely that the best sites for expansion have all been filled yet. Second, there is research to suggest that socioeconomic drivers

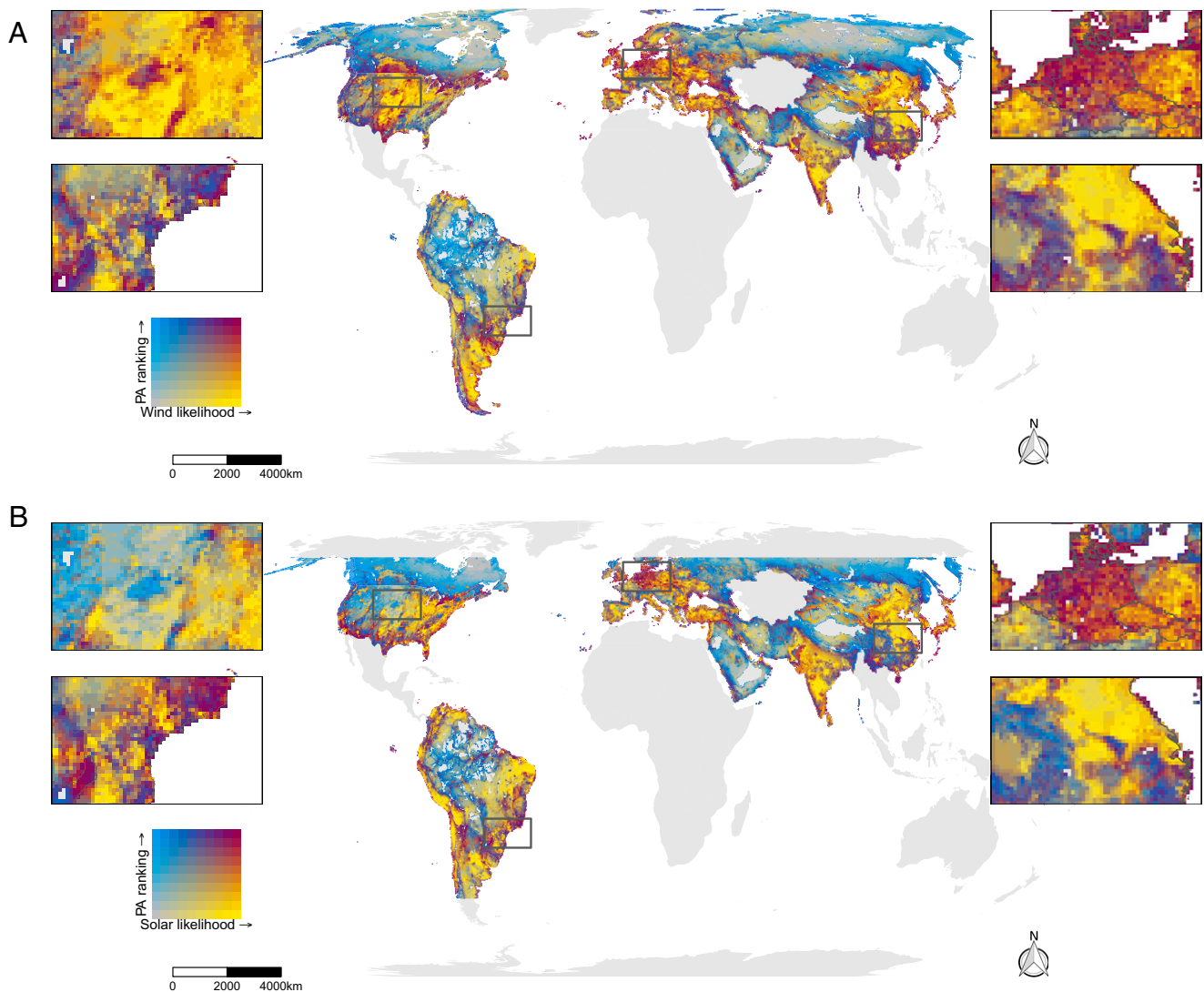


Fig. 1. Wind (A) and solar PV (B) likelihood versus PA priority expansion rankings. Wind and solar PV likelihood is the predicted probability (0 to 1) that an energy installation is present in a given grid cell. Probabilities represent the output of RF classification models trained on a spatially explicit global wind and solar PV database for the year 2020 and a suite of biophysical and socioeconomic predictors. Models were run for regions with more than 100 installations recorded; regions with fewer than 100 are excluded. PA priority expansion rankings are from a previous study that used spatial prioritization software to rank global cells (0 to 1, low to high) using species richness, ecoregion, and extinction risk. Current PAs and cells containing a wind or solar PV installation are excluded. Note: Input data were aggregated to 30-km² resolution for readability; the values appear truncated at extreme latitudes for solar because the underlying global horizontal irradiance data do not provide values for these regions.

cause renewable energy to become clumped in “hazard havens” where planning permission for projects is more likely for those close to other similar developments (47, 51). However, caution is required: As competition for land becomes even more intense, more research will be needed to assess whether predictors have shifted. This will become easier to assess as the renewable energy estate matures and time series analyses are possible in the same way as they now are for agriculture, in which recent cropland expansion has been shown to differ significantly from historic expansion (50). It may also open up regions excluded here to analysis; current data limitations introduce significant geographical bias here. While our study regions do cover a wide range of renewable energy and PA coverage (e.g., PA coverage is 18% in Central Europe and 2.6% in Middle East), significant differences between regions’ predictors suggest that results here cannot be extrapolated to, for example, regions in Africa. More research will be needed as renewable energy infrastructure in these regions proliferates.

More generally, our RFP models produced here refute suggestions that overlap between energy resource potential and priority PA expansion areas necessarily promotes conflict between the two (35). Renewable energy installations operate in complex environmental and socioeconomic envelopes that cannot be easily predicted on resource potential alone. The World Resources Institute Global Power Plant Database, which provides data on commissioning years (1896 to 2019) for a host of energy installations, provides further evidence that the threat of renewable energy to conservation areas globally is not increasing. Some renewable energy plants (wind and other renewables—hydro, geothermal, and biomass) do present generally higher proportions of overlap with conservation areas than conventional fuels (*SI Appendix, Fig. S2*). This could also be an underestimation; the authors highlight that wind and solar plants in the database cover only 49.48 and 21.03% of global installed capacity compared to >80% for conventional fuels. However, despite huge increases in the number of renewable energy plants and PAs,

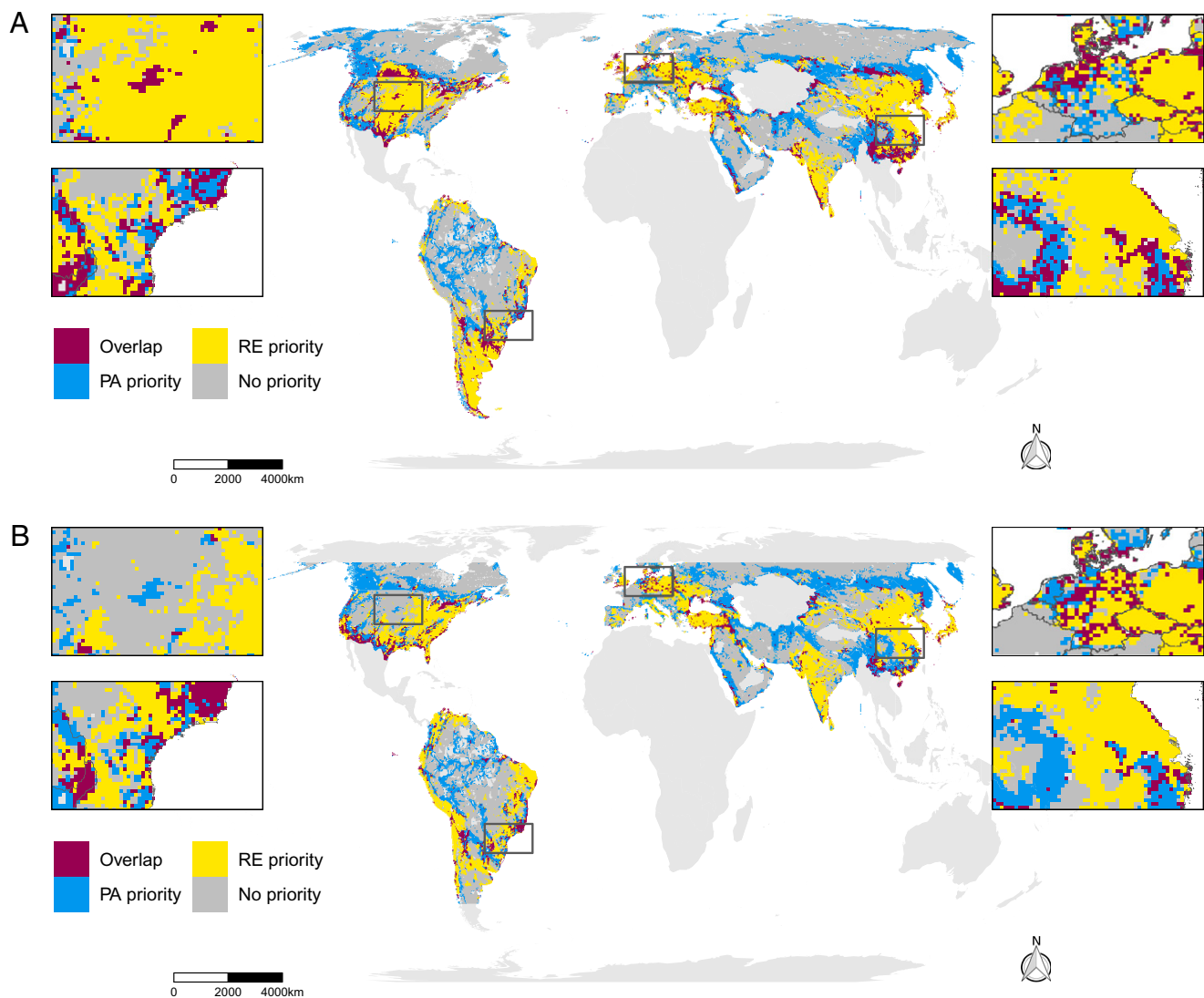


Fig. 2. Overlap between the top 30% land for wind (A) and solar PV (B) energy and the top 30% land for PA priority expansion. The top 30% land for wind and solar PV energy comprise the top 30% most likely cells to contain a wind or solar PV installation outside cells already containing one. This predicted probability is the output of RF classification models trained on a spatially explicit global wind and solar PV database for the year 2020 and a suite of biophysical and socioeconomic predictors including wind speed and global horizontal irradiance. Models were run for regions with more than 100 installations recorded; regions with fewer than 100 are excluded. The top 30% land for PA priority expansion comprises the top 30% ranked cells outside of cells already protected. The ranking was developed by a previous study to maximize coverage of species richness, species threat, and ecoregions. Note: Input data were aggregated to 30-km² resolution for readability; the values appear truncated at extreme latitudes for solar because the underlying global horizontal irradiance data do not provide values for these regions. RE, renewable energy.

the percentage overlap has remained relatively constant over time. Moreover, for three out of four wind and solar overlaps, the PA was designated after the installation was commissioned (*SI Appendix, Fig. S2B*).

Our results also bring important additional context to the question of the degree of current overlaps of wind and solar infrastructure and conservation areas. Our simple overlap results corroborate similar studies (*SI Appendix, Fig. S1 and Table S1*) (33). While the exact impacts of renewable energy technologies on biodiversity are far from well known, bird and bat mortality of wind turbines is one of the most evidenced impacts (28). As such, it is of concern that 1,090 utility-scale wind installations currently occur in KBAs, 79.69% of which are specifically designated as Important Bird and Biodiversity Areas (IBAs), a network of sites that are significant for the long-term viability of naturally occurring bird populations. Recently released IUCN guidance for wind and solar project developers details ways to

minimize infrastructure impacts on biodiversity and local communities, including avoidance of KBAs (52).

It is important to frame any overlap analysis in the context of land areas, especially when PAs make up ~14.41% of global land area, KBAs 13.9%, and wilderness areas 20.17%. A country with limited land area, a large PA network, and extensive renewable energy infrastructure would find it much harder to limit the overlap than one that was land rich. This is exemplified by most absolute overlaps occurring in Southern, Northern, and Central Europe, regions with large renewable energy estates and an extensive PA network compared with their size. That said, Brazil's high level of overlap, both absolute and relative to areas, is potentially worrying as it is one of the world's most species-rich countries, with a fast-growing economy (53).

While the number of overlaps with wilderness areas presented here was too small to provide a useful sample for modeling, the numbers roughly correspond to previous studies: Five

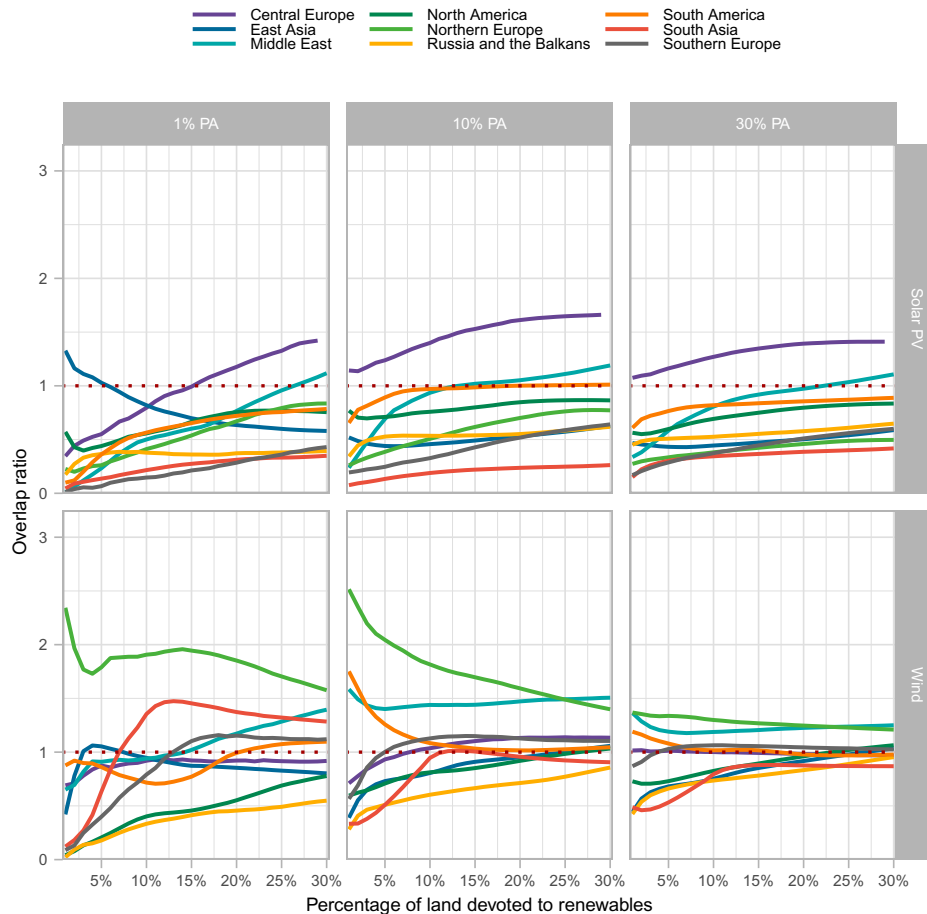


Fig. 3. Overlap ratios for the top priority renewable energy (RE) and PA priority expansion areas. For a given static extent of top PA priority expansion area (1, 10, or 30% of a region’s land area, labeled 1% PA, 10% PA, and 30% PA, respectively), cells with the highest likelihood for each RE technology are added cell by cell and the overlap ratio calculated until RE cells comprise 30% of the region area. Overlap ratios give an indication of the representativeness of overlapping priorities, given their occurrence in the wider landscape; a value of 1 would denote that PA priority expansion areas occur inside priority RE areas in the same proportions as they occur in the wider landscape. Values over 1 indicate spatial co-occurrence is over-represented (more common than expected), and values under 1 indicate less overlap than expected. For the *Top Leftmost* panel, 15% along the x axis would illustrate the overlap ratio for the top 15% solar PV areas and the top 1% PA priority expansion areas.

of the seven wilderness overlaps occur in North America and East Asia. This is a surprisingly low figure, especially considering wilderness areas in North America alone represent 8.513 million km² of undeveloped land, and previous research has suggested that energy infrastructure encroachment into wilderness areas may threaten previously untouched biodiversity (8, 33, 34, 54, 55). For comparison, the 2.562 million km² of PAs in the United States and Canada contain 173 overlapping installations. The dearth of installations in North America’s large expanse of wilderness, as defined by (38) and used in (33), may be a reflection of the technical difficulties of remote renewable power; previous studies have had to heavily constrain renewable suitability layers by distance to settlements to account for this (35, 54), whereas others have questioned the feasibility of some renewable projections on account of weak transmission and ancillary service proposals (56).

It has also been suggested that renewable energy expansion may threaten important conservation areas through PADD; Rehbein et al. (33), citing Mascia and Pailler (57) and Symes et al. (58), suggest that installations within strict PAs “strongly predict subsequent [PADD], which leads to worse biodiversity outcomes” (p. 3047). However, the results here, using the best available PADD data (59), did not identify any PADD events that were irrefutably caused by the siting of renewable

energy installations. Moreover, with 1,354 instances of well-established renewable energy installations in PAs, six instances is a small figure (0.517%). Of course, renewable energy installations could be a contributing factor to one of the other primary causes of PADD—for example, industrial-scale resource extraction and development or local land pressure and claims (59)—but currently there is no way of adequately testing this assertion. Regardless, best evidence suggests that renewable energy installations per se do not predict subsequent PADD.

Conclusion

Overall, our analyses suggest that future expansion of renewables and PAs are possible at regional scale with relatively little overlap. This finding is supported by our results that show—if land areas are considered—that current levels of overlap between wind, solar, and important conservation areas, while unfortunate, are not disproportionately large. Furthermore, there is some evidence to suggest they are also not increasing. Careful land use zoning is still very much required, particularly in densely populated regions such as Europe, and it is still unclear what the effects of a much more expansive extension in required areas would be. However, our results are encouraging as they suggest, for the regions considered and in the near term, that the vital

rollout of renewable energy infrastructure required to meet climate objectives could proceed in a way that does not present a major threat to area-based conservation efforts.

Materials and Methods

Renewable Energy Data. The spatially explicit wind and solar data represent 12,581 and 12,043 installations worldwide in 153 countries, totaling 322.8 and 125.6 GW of capacity, respectively (36). They currently represent the best available data for wind and solar infrastructure globally. These datasets were created by extracting features from OpenStreetMap and applying a spatial clustering algorithm. Data were filtered as suggested by the authors; installations not tagged as “water,” solar installations over 1 ha in area, and wind installations with greater than four turbines, except we did include installations tagged as “urban.” Wind and solar PV DPLs were taken from a study that produced gridded 1-km² resolution indices using multicriteria decision analyses that took into account resource potential and development feasibility (34).

Initial assessment of the DPLs showed that globally, 21.56% of installations in the spatially explicit data are present in grid cells that were classified as unsuitable for development of that renewable energy at 1-km² resolution, e.g., with a steep slope or high elevation (>30% or >3,000 m, respectively) (ref. 34, online-only table 2). This suggests the DPL approach is missing some installations when masking out unsuitable land at 1 km², either because renewable energy installations exist at a smaller spatial scale than 1 km² or the constraints imposed do not actually constrain renewable energy development, e.g., installations can exist where elevation >3000 m.

We also obtained an independent validation dataset: the Global Power Plant Database (GPPD) version 1.2.0 from the World Resources Institute, available at <https://datasets.wri.org/dataset/globalpowerplantdatabase>. This was used without modification.

Biodiversity Conservation. PA data used were from the December 2019 release of the World Database on Protected Areas (WDPA) (60). PA data were processed according to accepted practice (33, 37, 61, 62). Point locations for PAs were excluded, as well as polygons <5 km² in reported area. Only terrestrial PAs were considered and those with status Designated, Inscribed, or Established. We also obtained data on KBAs (September 2019 iteration) (63). KBAs are designated by the IUCN and signify sites contributing significantly to the global persistence of biodiversity. As with PAs, we excluded KBAs with only point data as well as those designated as marine IBAs. Areas of “wilderness” were collected from a previous study (38) identifying the remaining large, conterminous areas of the world with the lowest human footprint. The areas identified were split by country but otherwise used without modification.

Priority expansion areas for PAs were obtained from a previous study looking to assess the effects of land change and national versus global priorities on the efficacy of the global PA estate, obtained from <https://www.fairdata.fi/avaal/> (37). This study used range maps of all threatened terrestrial vertebrates identified by the IUCN Red List of Threatened Species at the time (24,757 species globally) and the world’s 827 World Wildlife Fund ecoregions. The analysis took the 2013 PA network and identified areas outside these that represented the best opportunities for expansion, with rankings weighted on species numbers and ecoregion representativeness using the conservation spatial planning tool Zonation (version 4). The data are available at 0.008333° resolution, WGS84 projection. They ran two allocation scenarios to expand PAs to given thresholds: one that ranked cells globally and one that ranked cells nationally. For each of these scenarios, they discounted these expansion areas by projected land change to 2040, resulting in four overall scenarios: global designation with 2040 land use, global designation with 2000 land use, national designation with 2040 land use, and national designation with 2000 land use. In order to correctly use the PA priority expansion rankings, we used archive WDPA data from June 2013. As mentioned in Rehbein et al. (33), China has since removed a large portion of its PA estate from the WDPA, and a very large PA in Saudi Arabia was significantly downsized between 2013 and 2019. The spatial prioritization process described in Pouzols et al. (37) ranked PAs present in June 2013 with the highest ranking. Unless masked out with the archive WDPA data, the disappearance of these large PAs between June 2013 and December 2019 would lead to artifacts of artificially high rankings in the global grid; this was corrected through the combined use of PA data from June 2013 and December 2019.

Data on PADD were downloaded from PADDTRACKER (available at <https://www.paddtracker.org/>). These data were collated in a study that originally identified 3,749 PADD events (59). Between 1892 and 2018, 519,857 km² has been removed from protection, with 1.660 million km² downgraded. For the purposes of this (spatial) study, these data were filtered by events with

known locations, as recommended by the authors. This stipulation removed 61 events. As with other conservation data, events with point data were excluded; this exclusion removed 23.89% of the total area affected by PADD events. Furthermore, events were filtered by the event cause: only events where the cause was identified as “Infrastructure” were included. This generated six PADD events of interest, totaling 24.84 km². As the figure was so low, we elected to include previously excluded point data, buffered to their reported areas. This added a final two events.

Creation of the Wind and Solar PV Potential Layers. We evaluated both the PA priority expansion data and renewable energy DPLs for their ability to predict occurrences (*SI Appendix*). While the PA priority expansion data performed well, the DPLs did not. Regional wind and solar PV RFP layers were therefore created using the *zoon* and *raster* R packages (64, 65). The *zoon* package allows users to create reproducible workflows for distribution modeling. For the observed occurrence of renewable energy facilities, we use a spatially explicit global database of wind and solar PV (36). With no formal absence data and because group discrimination species distribution models (those with presence/absence data) tend to perform better than profile methods (presence only) (65–67), we looked to generate sensible pseudoabsences, a well-established technique in species distribution modeling (68, 69). While previous studies create probability layers by layering constraints atop resource potential maps, this method uses no constraints except for land surface and allows us to scrutinize what drives the distribution of the renewable energy estate. We chose RF models over two similar methods because it showed better accuracy in preliminary tests, even without the parameter tuning RFs can implement (*SI Appendix, Fig. S8*). World regions with >100 observations of wind and solar PV occurrences were selected. The rationale for this is that we consider 10 predictor variables and wanted to maintain a ratio of at least 10 events per predictor variable (as this ratio has been shown to function as a useful threshold for logistic regression, e.g., classification) (70). These regions were Middle East, Southern Europe, South America, North America, South Asia, Russia and the Balkans, East Asia, Northern Europe, and Central Europe with sample sizes ranging from 145 to 3,639. We used a ratio of 1:1 pseudoabsence points to presence points, as suggested by Barbet-Massin et al. (68) for classification models such as RF. This led to our threshold for classifying a presence being 0.5. Performance metrics were calculated using 10-fold, 5-repeat cross validation in the first instance. Furthermore, to enable a fair comparison of the DPLs with our created RFP layers, we tested the predictive power of both indicators against an independent dataset of wind and solar powerplants (*SI Appendix, Fig. S2*), the GPPD (*Renewable Energy Data*).

The following global datasets were used in which all were reprojected, and in some cases aggregated, to Mollweide equal-area projection, 1-km² resolution for the RF analysis to create the RFP layers:

- 2015 accessibility (travel time to cities) (71);
- 2005 gridded data of cattle, goats, and sheep derived from the Gridded Livestock of the World datasets (72);
- 2005 cropland percentage per pixel (73);
- Elevation (and calculated slope), available from <http://viewfinderpanoramas.org/dem3.html>;
- Gridded distance from PAs, calculated from the protected area data described above;
- 2015 population density from the Gridded Population of the World version 4 (74);
- Total road density from the Global Roads Inventory Project dataset (originally in WGS84 0.08333° resolution and simply disaggregated to 0.008333° resolution) (75);
- Global horizontal irradiance from the Global Solar Atlas, available from <https://globalsolaratlas.info/>; and
- Global wind speed at 100m height from the Global Wind Atlas, available from <https://globalwindatlas.info/>.

Bivariate Global Grids. To present the relationship between our wind and solar PV RFP layers and the PA priority expansion rankings, we created global bivariate grids. The PA priority expansion layer (global 2040 land use scenario) was masked with current protected cells at 1-km² resolution as well as the archive data from June 2013 at 1-km² resolution, and the solar PV and wind RFP layers were masked with current wind and solar installations at 1-km² resolution. Global bivariate grids were created by reclassifying input raster data into 10 bins of equal representation and then combining each RFP layer with the PA priority expansion layer to create global grids with 100 unique values. For plotting, the process was identical, except the input raster data were aggregated with bilinear interpolation to 30 km² and projected to an Eckert IV equal area.

Overlap Ratios. We calculated the ratio of overlap of top priority PA expansion areas and renewable energy areas (50, 76). Overlap ratios enable like-for-like comparisons of overlaps between two binary responses (PA and energy in this case) for different areas and indicate if overlaps are over-represented (>1) or under-represented (<1) given the land available. For a given static threshold of PA priority area (1, 10, or 30% of total land area), we iteratively added the highest-ranking renewable energy RFP cell within the region until coverage reached 30%. At every step, we calculated the overlap ratio by dividing the percentage of PA priority cells that overlap priority renewable energy areas by the percentage of total land covered by priority renewable energy areas. For example, if 20% of PA priority areas overlap with priority renewable energy areas and priority renewable energy areas cover 30% of a region, then the ratio is $0.2/0.3 = 0.66$. If, however, 40% of PA priority areas overlapped with priority renewable energy areas covering 30% of a region, the ratio is $0.4/0.3 = 1.25$. See *SI Appendix, Fig. S12* for a graphical explanation of overlap ratios.

Spatial Overlaps. Spatial overlaps were conducted using two different methodologies. The first looked at absolute overlaps. Simple spatial overlaps of renewable energy installations and conservation areas were performed using the *sf* and *raster* R packages. Data were reprojected to Mollweide equal-area projection to ensure comparability of areas at all latitudes. Spatial overlaps were based on the predicate *st_contains_properly*, a function that ensures only installations completely contained within conservation areas were considered. This was done to minimize the risk of boundary

inaccuracies flagging false overlaps where an installation and a conservation area merely intersect each other.

The second overlap methodology looked at overlaps relative to the area of renewable energy and conservation priority in each country. We fitted simple linear models: $\text{overlap area} \sim \text{renewable area} + \text{conservation area} + \text{land area}$ per country (*SI Appendix, Tables S3, S6, and S7*); countries with large positive standardized residuals are those with more renewable infrastructure overlapping conservation areas than predicted relative to other countries with similar PA and renewable energy estates.

A simple absolute overlap process was also performed for renewable energy installations and the PADD events of interest. However, as point data comprised a significant portion of these data (27.9%), we opted to include buffered point data in this analysis; the radii for the circular buffers were calculated from the reported area of the PADD event.

Data Availability. All data resulting from the analyses have been deposited in Figshare, DOI: [10.6084/m9.figshare.15062550](https://doi.org/10.6084/m9.figshare.15062550). Previously published data were used for this work (34, 36, 37).

ACKNOWLEDGMENTS. We are grateful for helpful comments from Alona Armstrong and Jim Wright on an early draft and thank the (often unsung) data curators of the respective conservation datasets, especially Edward Lewis for sourcing the archive WDPA data. We also thank two anonymous reviewers for significant improvements to our manuscript. Funding was provided by Addressing the Valuation of Energy and Nature Together Grant/Award NE/M019640/1, Natural Environment Research Council (NERC), and a University of Southampton studentship to S.D.

1. United Nations Framework Convention on Climate Change, *Draft Decision: CP.21, FCCC/CP/2015/L.9/Rev.1*. (2015). unfccc.int/resource/docs/2015/cop21/eng/09r01.pdf. Accessed 8 January 2022..
2. International Renewable Energy Agency, "Global renewables outlook: Energy transformation 2050" (2020). <https://www.irena.org/publications/2020/Apr/Global-Renewables-Outlook-2020>. Accessed 8 January 2022.
3. International Renewable Energy Agency, "Renewable energy highlights" (2020). https://www.irena.org/-/media/Files/IRENA/Agency/Publication/2020/Jul/Renewable_energy_highlights_July_2020.pdf?la=en&hash=75B114DB7A55F4260F41F64C4DF793DB2044306. Accessed 8 January 2022.
4. U. R. Fritsche *et al.*, "Global Land Outlook Working Paper: Energy and land use" (United Nations Convention to Combat Desertification, 2017). <https://doi.org/10.13140/RG.2.2.24905.44648>. Accessed 11 January 2022.
5. V. Smil, *Energy in Nature and Society: General Energetics of Complex Systems* (MIT Press, 2008).
6. J. van Zalk, P. Behrens, The spatial extent of renewable and non-renewable power generation: A review and meta-analysis of power densities and their application in the U.S. *Energy Policy* **123**, 83–91 (2018).
7. L. M. Miller, D. W. Keith, Observation-based solar and wind power capacity factors and power densities. *Environ. Res. Lett.* **13**, 104008 (2018).
8. A. M. Trainor, R. I. McDonald, J. Fargione, Energy sprawl is the largest driver of land use change in United States. *PLoS One* **11**, e0162269 (2016).
9. United Nations Convention to Combat Desertification, "Energy and climate" in *The Global Land Outlook*, N. Dudley, S. Alexander, Eds. (United Nations Convention to Combat Desertification, ed. 1, 2017), pp. 212–225.
10. V. Smil, "Power density primer: Understanding the spatial dimension of the unfolding transition to renewable electricity generation." *MasterResource* (2010). <https://www.masterresource.org/smil-vaclav/smil-density-definitions-ii>. Accessed 8 January 2022.
11. R. A. Holland *et al.*, The influence of the global electric power system on terrestrial biodiversity. *Proc. Natl. Acad. Sci. U.S.A.* **116**, 26078–26084 (2019).
12. T. D. Searchinger, T. Beringer, A. Strong, Does the world have low-carbon bioenergy potential from the dedicated use of land? *Energy Policy* **110**, 434–446 (2017).
13. R. Slade, R. Saunders, R. Gross, A. Bauen, "Energy from biomass: The size of the global resource" (Imperial College Centre for Energy Policy and Technology and UK Energy Research Centre, 2011).
14. S. Fuss *et al.*, Negative emissions—Part 2: Costs, potentials and side effects. *Environ. Res. Lett.* **13**, 063002 (2018).
15. International Renewable Energy Agency, "Future of wind: Deployment, investment, technology, grid integration and socio-economic aspects" (IRENA, 2019).
16. R. R. Hernandez, M. K. Hoffacker, M. L. Murphy-Mariscal, G. C. Wu, M. F. Allen, Solar energy development impacts on land cover change and protected areas. *Proc. Natl. Acad. Sci. U.S.A.* **112**, 13579–13584 (2015).
17. D. A. Eitelberg, J. van Vliet, P. H. Verburg, A review of global potentially available cropland estimates and their consequences for model-based assessments. *Glob. Change Biol.* **21**, 1236–1248 (2015).
18. T. Iizumi *et al.*, Responses of crop yield growth to global temperature and socioeconomic changes. *Sci. Rep.* **7**, 7800 (2017).
19. R. Seppelt, A. M. Manceur, J. Liu, E. P. Fenichel, S. Klotz, Synchronized peak-rate years of global resources use. *Ecol. Soc.* **19**, 50 (2014).
20. E. Dinerstein *et al.*, An ecoregion-based approach to protecting half the terrestrial realm. *Bioscience* **67**, 534–545 (2017).
21. S. Baruch-Mordo, J. M. Kiesecker, C. M. Kennedy, J. R. Oakleaf, J. J. Opperman, From Paris to practice: Sustainable implementation of renewable energy goals. *Environ. Res. Lett.* **14**, 024013 (2019).
22. J. Kiesecker *et al.*, Hitting the target but missing the mark: Unintended environmental consequences of the Paris climate agreement. *Front. Environ. Sci.* **7**, 151 (2019).
23. J. Köppel, M. Dahmen, J. Helfrich, E. Schuster, L. Bulling, Cautious but committed: Moving toward adaptive planning and operation strategies for renewable energy's wildlife implications. *Environ. Manage.* **54**, 744–755 (2014).
24. A. Gasparatos, C. N. H. Doll, M. Esteban, A. Ahmed, T. A. Olang, Renewable energy and biodiversity: Implications for transitioning to a Green Economy. *Renew. Sustain. Energy Rev.* **70**, 161–184 (2017).
25. L. Gibson, E. N. Wilman, W. F. Laurance, How green is 'green' energy? *Trends Ecol. Evol.* **32**, 922–935 (2017).
26. R. Miao, P. N. Ghosh, M. Khanna, W. Wang, J. Rong, Effect of wind turbines on bird abundance: A national scale analysis based on fixed effects models. *Energy Policy* **132**, 357–366 (2019).
27. E. Schuster, L. Bulling, J. Köppel, Consolidating the state of knowledge: A synoptical review of wind energy's wildlife effects. *Environ. Manage.* **56**, 300–331 (2015).
28. C. B. Thaxter *et al.*, Bird and bat species' global vulnerability to collision mortality at wind farms revealed through a trait-based assessment. *Proc. Biol. Sci.* **284**, 20170829 (2017).
29. M. Thompson, J. A. Beston, M. Etterson, J. E. Diffendorfer, S. R. Loss, Factors associated with bat mortality at wind energy facilities in the United States. *Biol. Conserv.* **215**, 241–245 (2017).
30. R. R. Hernandez *et al.*, Environmental impacts of utility-scale solar energy. *Renew. Sustain. Energy Rev.* **29**, 766–779 (2014).
31. J. E. Lovich, J. R. Ennen, Assessing the state of knowledge of utility-scale wind energy development and operation on non-volant terrestrial and marine wildlife. *Appl. Energy* **103**, 52–60 (2013).
32. K. A. Moore-O'Leary *et al.*, Sustainability of utility-scale solar energy — Critical ecological concepts. *Front. Ecol. Environ.* **15**, 385–394 (2017).
33. J. A. Rehbein *et al.*, Renewable energy development threatens many globally important biodiversity areas. *Glob. Chang. Biol.* **26**, 3040–3051 (2020).
34. J. R. Oakleaf *et al.*, Mapping global development potential for renewable energy, fossil fuels, mining and agriculture sectors. *Sci. Data* **6**, 101 (2019).
35. A. Santangeli *et al.*, Global change synergies and trade-offs between renewable energy and biodiversity. *Glob. Change Biol. Bioenergy* **8**, 941–951 (2015).
36. S. Dunnett, A. Sorichetta, G. Taylor, F. Eigenbrod, Harmonised global datasets of wind and solar farm locations and power. *Sci. Data* **7**, 130 (2020).
37. F. M. Pouzols *et al.*, Global protected area expansion is compromised by projected land-use and parochialism. *Nature* **516**, 383–386 (2014).
38. J. R. Allan, O. Venter, J. E. M. Watson, Temporally inter-comparable maps of terrestrial wilderness and the Last of the Wild. *Sci. Data* **4**, 170187 (2017).
39. A. Scheidel, A. H. Sorman, Energy transitions and the global land rush: Ultimate drivers and persistent consequences. *Glob. Environ. Change* **22**, 588–595 (2012).
40. N. Dudley, P. Shadie, S. Stolton, *Guidelines for Applying Protected Area Management Categories*, N. Dudley, Ed. (International Union for Conservation of Nature, 2013).
41. J. M. Kiesecker *et al.*, Win-win for wind and wildlife: A vision to facilitate sustainable development. *PLoS One* **6**, e17566 (2011).

42. N. Butt *et al.*, Biodiversity risks from fossil fuel extraction. *Science* **342**, 425–426 (2013).
43. M. B. J. Harfoot *et al.*, Present and future biodiversity risks from fossil fuel exploitation. *Conserv. Lett.* **11**, e12448 (2018).
44. C. McGlade, P. Ekins, The geographical distribution of fossil fuels unused when limiting global warming to 2 °C. *Nature* **517**, 187–190 (2015).
45. S. Szopa *et al.*, “Short-lived climate forcers” in *Climate Change 2021: The Physical Science Basis. Contribution of Working Group I to the Sixth Assessment Report of the Intergovernmental Panel on Climate Change*, V. Masson-Delmotte *et al.*, Eds. (Cambridge University Press, 2021).
46. P. R. Elsen, W. B. Monahan, E. R. Dougherty, A. M. Merenlender, Keeping pace with climate change in global terrestrial protected areas. *Sci. Adv.* **6**, eaay0814 (2020).
47. P. Roddis, S. Carver, M. Dallimer, P. Norman, G. Ziv, The role of community acceptance in planning outcomes for onshore wind and solar farms: An energy justice analysis. *Appl. Energy* **226**, 353–364 (2018).
48. M. Harper, B. Anderson, P. A. B. James, A. S. Bahaj, Onshore wind and the likelihood of planning acceptance: Learning from a Great Britain context. *Energy Policy* **128**, 954–966 (2019).
49. E. C. Ellis *et al.*, Used planet: A global history. *Proc. Natl. Acad. Sci. U.S.A.* **110**, 7978–7985 (2013).
50. F. Eigenbrod *et al.*, Identifying agricultural frontiers for modeling global cropland expansion. *One Earth* **3**, 504–514 (2020).
51. A. Blowers, *Planning for a Sustainable Environment* (Routledge, 2013).
52. L. Bennun *et al.*, *Mitigating Biodiversity Impacts Associated with Solar and Wind Energy Development: Guidelines for Project Developers* (International Union for Conservation of Nature, 2021), <https://doi.org/10.2305/IUCN.CH.2021.04.en>.
53. R. A. Mittermeier, C. G. Mittermeier, P. Robles Gil, *Megadiversity: Earth's Biologically Wealthiest Nations* (CEMEX, English ed. 1, 1997).
54. A. Santangeli *et al.*, Synergies and trade-offs between renewable energy expansion and biodiversity conservation — A cross-national multifactor analysis. *Glob. Change Biol. Bioenergy* **8**, 1191–1200 (2016).
55. W. F. Laurance, I. B. Arrea, Roads to riches or ruin? *Science* **358**, 442–444 (2017).
56. B. P. Heard, B. W. Brook, T. M. L. Wigley, C. J. A. Bradshaw, Burden of proof: A comprehensive review of the feasibility of 100% renewable-electricity systems. *Renew. Sustain. Energy Rev.* **76**, 1122–1133 (2017).
57. M. B. Mascia, S. Pailler, Protected area downgrading, downsizing, and degazettement (PADDD) and its conservation implications. *Conserv. Lett.* **4**, 9–20 (2011).
58. W. S. Symes, M. Rao, M. B. Mascia, L. R. Carrasco, Why do we lose protected areas? Factors influencing protected area downgrading, downsizing and degazettement in the tropics and subtropics. *Glob. Change Biol.* **22**, 656–665 (2016).
59. R. E. Golden Kroner *et al.*, The uncertain future of protected lands and waters. *Science* **364**, 881–886 (2019).
60. UNEP-WCMC and IUCN, Protected Planet: The World Database on Protected Areas (WDPA) [Online]. (UNEP-WCMC and IUCN, Cambridge, UK, 2019). www.protectedplanet.net. Accessed 11 January 2022.
61. UNEP-WCMC, “Calculating protected area and OECM coverage” *Protected Planet* (17 May 2021). <https://www.protectedplanet.net/en/resources/calculating-protected-area-coverage>. Accessed 8 January 2022.
62. P. Visconti *et al.*, Effects of errors and gaps in spatial data sets on assessment of conservation progress. *Conserv. Biol.* **27**, 1000–1010 (2013).
63. BirdLife International. *The World Database of Key Biodiversity Areas*. Developed by the KBA Partnership: BirdLife International, International Union for the Conservation of Nature, Amphibian Survival Alliance, Conservation International, Critical Ecosystem Partnership Fund, Global Environment Facility, Global Wildlife Conservation, NatureServe, Rainforest Trust, Royal Society for the Protection of Birds, Wildlife Conservation Society and World Wildlife Fund. (2019). www.keybiodiversityareas.org. Accessed 1 September 2019.
64. R. J. Hijmans, raster: Geographic data analysis and modeling. R package version 2.6-7 (2017). <https://CRAN.R-project.org/package=raster>. Accessed 8 January 2022.
65. N. Golding *et al.*, The zoon R package for reproducible and shareable species distribution modelling. *Methods Ecol. Evol.* **9**, 260–268 (2018).
66. J. Elith *et al.*, Novel methods improve prediction of species' distributions from occurrence data. *Ecography* **29**, 129–151 (2006).
67. F. G. Barbosa, F. Schneck, Characteristics of the top-cited papers in species distribution predictive models. *Ecol. Modell.* **313**, 77–83 (2015).
68. M. Barbet-Massin, F. Jiguet, C. H. Albert, W. Thuiller, Selecting pseudo-absences for species distribution models: How, where and how many? *Methods Ecol. Evol.* **3**, 327–338 (2012).
69. C. Liu, G. Newell, M. White, The effect of sample size on the accuracy of species distribution models: Considering both presences and pseudo-absences or background sites. *Ecography* **42**, 535–548 (2019).
70. P. Peduzzi, J. Conato, E. Kemper, T. R. Holford, A. R. Feinstein, A simulation study of the number of events per variable in logistic regression analysis. *J. Clin. Epidemiol.* **49**, 1373–1379 (1996).
71. D. J. Weiss *et al.*, A global map of travel time to cities to assess inequalities in accessibility in 2015. *Nature* **553**, 333–336 (2018).
72. T. P. Robinson *et al.*, Mapping the global distribution of livestock. *PLoS One* **9**, e96084 (2014).
73. S. Fritz *et al.*, Mapping global cropland and field size. *Glob. Change Biol.* **21**, 1980–1992 (2015).
74. E. Doxsey-Whitfield *et al.*, Taking advantage of the improved availability of census data: A first look at the gridded population of the world, version 4. *Pap. Appl. Geogr.* **1**, 226–234 (2015).
75. J. R. Meijer, M. A. J. Huijbregts, K. C. G. J. Schotten, A. M. Schipper, Global patterns of current and future road infrastructure. *Environ. Res. Lett.* **13**, 064006 (2018).
76. F. Eigenbrod *et al.*, Ecosystem service benefits of contrasting conservation strategies in a human-dominated region. *Proc. Biol. Sci.* **276**, 2903–2911 (2009).